
Classification of Superstatistical Features in High Dimensions

Urte Adomaityte
Department of Mathematics
King's College London
urte.adomaityte@kcl.ac.uk

Gabriele Sicuro
Department of Mathematics
King's College London
gabriele.sicuro@kcl.ac.uk

Pierpaolo Vivo
Department of Mathematics
King's College London
pierpaolo.vivo@kcl.ac.uk

Abstract

We characterise the learning of a mixture of two clouds of data points with generic centroids via empirical risk minimisation in the high dimensional regime, under the assumptions of generic convex loss and convex regularisation. Each cloud of data points is obtained by sampling from a possibly uncountable superposition of Gaussian distributions, whose variance has a generic probability density ϱ . Our analysis covers therefore a large family of data distributions, including the case of power-law-tailed distributions with no covariance. We study the generalisation performance of the obtained estimator, we analyse the role of regularisation, and the dependence of the separability transition on the distribution scale parameters.

1 Introduction

Simple classification and regression tasks in high dimensions via generalised linear models (GLMs) exhibit a non-trivial phenomenology which is found to be similar to the one observed in over-parametrised deep neural networks [44, 19]. Random features models [39, 28, 13], for example, have provided an effective theoretical framework suitable for complete analytical treatment, which contributed to our understanding of the well-known double-descent phenomenon in neural networks [33, 3, 4]. In recent years, a large class of GLMs has been proposed to investigate a number of aspects of the problem of learning in high dimensions, benefiting from a long tradition of pioneering studies dating back to the last decade of the previous century [42, 47]. A crucial assumption in many such theoretical models is that the dataset is obtained from a *Gaussian* distribution. The Gaussian assumption has served as a convenient working hypothesis that, as we will discuss below, can be experimentally and theoretically justified in many simple contexts. However, such an assumption might considerably limit the scope of insights we can obtain from such models with respect to architectures trained on real-world data, which are, more often than not, non-Gaussian.

This paper presents, to the best of our knowledge for the first time, the exact asymptotics for classification tasks on a large family of heavy-tailed dataset distributions. We will focus on supervised binary classification assuming that the sample size n and the dimensionality d of the space where the data points live are both sent to infinity, keeping their ratio $n/d = \alpha$ fixed. The paper fits therefore in the line of works on exact high-dimensional asymptotics for classification learning via a GLM [30, 25], but, crucially, we relax the usual Gaussian hypothesis by including in our analysis power-law-tailed distributions with possibly no covariance. In particular, we will assume that each data points' cloud results from a *possibly uncountable* superposition of Gaussian distributions, each of

them with covariance $\Sigma = \Delta \mathbf{I}_d \in \mathbb{R}^{d \times d}$, where Δ is itself a random quantity with density ϱ . Using, for example, an inverse-Gamma distribution for ϱ , such *superstatistical* construction [1, 2] provides a fat-tailed data distribution [46] which, for a proper choice of ϱ , can result, for example, in a Cauchy-like, infinite variance density. The replica method [29], an analytical tool widely adopted in statistical physics, allows us to obtain asymptotic formulas for the test error and training error for this large family of distributions, allowing us to study the effects of non-Gaussianity on the performance curves and test the Gaussian universality hypothesis [38] in such a classification task.

Motivation and related works Learning a rule to classify data points clustered in clouds in high dimension is a classical problem in statistics [18]. Its ubiquity is exemplified by the recently observed neural collapse phenomenon in deep neural networks, in which the last layer classifier is found to operate on features clustered in clouds around the vertices of a simplex [21, 35]; more recently, Seddik et al. [41] showed that Gaussian mixtures suitably describe the deep learning representation of GAN data. In theoretical models, data points are typically assumed to be organised in K *Gaussian* clouds, each one of them corresponding to a class. Each class k , $k \in \{1, \dots, K\}$, is centered around a mean vector μ_k and has covariance Σ_k . The binary classification case, $K = 2$, is the simplest, and possibly most studied, setting. Mai and Liao [27] considered an ERM task with generic convex loss and ridge regularisation in the high-dimensional regime $n, d \rightarrow +\infty$ with $n/d \in (0, +\infty)$. In this setting, they gave a precise prediction of the classification error, showing the optimality of the square loss in the unregularized case. Their results have been extended by Mignacco et al. [30], who showed that the presence of a regularisation can actually drastically affect the performance, improving it. In the same setting, the Bayes optimal estimator has been studied in both the supervised and the semi-supervised setting [30, 24]. In the context of binary classification, the number n of samples that can be perfectly fitted by a linear model in dimension d [30, 8, 20] has been the topic of investigation since the seminal work of Cover [5] and is related to the classical storage capacity problems on networks [11, 12, 22]. The associated separability threshold value $\alpha = n/d$ is remarkably associated with the existence transition of the maximum likelihood estimator [44, 48]. Finally, Loureiro et al. [25] recently gave the precise asymptotic characterisation of the test error in learning to classify $K \geq 2$ Gaussian clouds with generic means and covariances.

As already mentioned, a widely adopted working hypothesis on the data points distribution in the considered classification problem is their *Gaussianity*. Beyond being a convenient theoretical hypothesis, such an assumption has been justified in terms of a ‘‘Gaussian universality’’ principle. In a number of circumstances, non-Gaussian distributions are found to be effectively described by Gaussian ones with matching first and second moments as far as the asymptotic properties of the estimators are concerned [26, 14]. Such a ‘‘universality property’’ has been rigorously proven for example in compressed sensing [31] or in the case of LASSO with non-Gaussian dictionaries [34]. A Gaussian equivalence principle has been introduced by Goldt et al. [16] and has been proven to hold for a wide class of generalised linear estimation problems [28, 14]. Yet it is also known that such universality can break down. For example, studying elliptic regression tasks on elliptical distribution, El Karoui [9] made evident that the statistics of the estimator can depend on higher moments of the dataset distribution [9, 43, 45]. More recently, Pesce et al. [38] showed that heteroscedasticity and the presence of data structure can destroy any form of ‘‘Gaussian equivalence’’ in the asymptotic error of GLMs. Building upon a series of contributions related to the asymptotic performance of models in the proportional high-dimensional limit [19, 28, 15, 13, 17, 26], we aim precisely to explore the validity of Gaussian universality within classification problems. In our work, we adopt the aforementioned ‘‘superstatistical setting’’ [1, 2] by considering a much larger family of distributions, including the case of power-law-tailed distributions with no covariance.

Our contributions In this manuscript we provide the following results.

- We study a classification task on a non-Gaussian mixture model in Eq. (1) below and we analytically derive, using the replica method [6, 10, 29], an asymptotic characterisation of the statistics of the empirical risk minimisation (ERM) estimator. Our results go beyond the usual Gaussian assumption and include for example the case of point clouds obtained from distributions with no variance. The analysis is performed in the high-dimensional, proportional limit and for any convex loss and convex regularisation. By using this result, we provide asymptotic formulas for the generalisation and training errors.
- We analyse the performance of such ERM task on a specific family of point distributions by using different convex loss functions (quadratic and logistic) and ridge regularisation. We show in particular

that, in the case of two balanced clusters with a specific non-Gaussian distribution, the optimal ridge regularisation strength λ^* is finite, at variance with the purely Gaussian case investigated by Mignacco et al. [30], for which $\lambda^* \rightarrow \infty$.

- We finally estimate the separability threshold on a large family of data point distributions, including the case of infinite-variance clouds, comparing our results to the known asymptotics for Gaussian clouds obtained by Mignacco et al. [30]. As expected, we recover the result of Cover [5] in the case of infinite distribution width.

2 Main result

Dataset construction We consider the task of classifying two data clusters in the d -dimensional space \mathbb{R}^d . The dataset $\mathcal{D} := \{(\mathbf{x}^\nu, y^\nu)\}_{\nu \in [n]}$ is obtained by extracting n independent datapoints \mathbf{x}^ν , each associated with a label $y^\nu \in \{-1, 1\}$. The point positions are correlated with the labels via a law $P(\mathbf{x}, y)$ which we assume to have the form

$$P(\mathbf{x}, y) = \delta_{y,1} \rho P(\mathbf{x}|\boldsymbol{\mu}_+) + \delta_{y,-1} (1 - \rho) P(\mathbf{x}|\boldsymbol{\mu}_-), \quad \rho \in (0, 1), \quad \boldsymbol{\mu}_\pm \in \mathbb{R}^d. \quad (1a)$$

Here $P(\mathbf{x}|\boldsymbol{\mu})$ is the distribution of a cloud having mean $\boldsymbol{\mu}$, and the mean vectors $\boldsymbol{\mu}_\pm \in \mathbb{R}^d$ are distributed according to some density, such that $\mathbb{E}[\|\boldsymbol{\mu}\|^2] = \Theta(1)$. The scalar quantity ρ weighs the relative contribution of the two clusters: in the following, we will denote $\rho_+ = \rho = 1 - \rho_-$. Each cluster distribution $P(\mathbf{x}|\boldsymbol{\mu})$ around a vector $\boldsymbol{\mu}$ is assumed to have the form

$$P(\mathbf{x}|\boldsymbol{\mu}) := \mathbb{E}_\Delta [\mathcal{N}(\mathbf{x}|\boldsymbol{\mu}, \Delta \mathbf{I}_d)], \quad (1b)$$

where $\mathcal{N}(\mathbf{x}|\boldsymbol{\mu}, \boldsymbol{\Sigma})$ is a Gaussian distribution with mean $\boldsymbol{\mu} \in \mathbb{R}^d$ and covariance $\boldsymbol{\Sigma} \in \mathbb{R}^{d \times d}$, and Δ is randomly distributed with some density $\varrho(\Delta)$ with support on \mathbb{R}^+ . The family of distributions in the form above has been extensively studied, for example, by the physics community, in the context of *superstatistics* [1, 2]. It includes a large class of distributions with properties markedly different from the ones of Gaussians. For example, the inverse-Gamma distribution $\varrho(\Delta) = (2\pi\Delta^3)^{-1/2} e^{-\frac{1}{2\Delta}}$ leads to a d -dimensional Cauchy-like distribution $P(\mathbf{x}|\boldsymbol{\mu}) \propto (1 - \|\boldsymbol{\mu} - \mathbf{x}\|^2)^{-\frac{d+1}{2}}$, having as marginals Cauchy distributions and $\mathbb{E}[\|\mathbf{x} - \boldsymbol{\mu}\|^2] = +\infty$. We will perform our classification task by searching for a set of parameters (\mathbf{w}^*, b^*) , called respectively *weights* and *bias*, that will allow us to construct an estimator via a certain classifier $\varphi: \mathbb{R} \rightarrow \{-1, 1\}$

$$\mathbf{x} \mapsto \varphi \left(\frac{\mathbf{w}^{*\top} \mathbf{x}}{\sqrt{d}} + b^* \right), \quad (2)$$

which will provide us with our prediction for a new, unseen data point \mathbf{x} sampled from the same law $P(\mathbf{x}, y)$. Our analysis will be performed in the high-dimensional limit where both the sample size n and dimensionality d are sent to infinity, with $n/d \equiv \alpha$ kept constant.

Learning task In the most general setting, the parameters are estimated by minimising an empirical risk function in the form

$$(\mathbf{w}^*, b^*) \equiv \arg \min_{\substack{\mathbf{w} \in \mathbb{R}^d \\ b \in \mathbb{R}}} \mathcal{R}(\mathbf{w}, b) \quad \text{where} \quad \mathcal{R}(\mathbf{w}, b) \equiv \sum_{\nu=1}^n \ell \left(y^\nu, \frac{\mathbf{w}^\top \mathbf{x}^\nu}{\sqrt{d}} + b \right) + \lambda r(\mathbf{w}). \quad (3)$$

Here ℓ is a strictly convex loss function with respect to its second argument, and r is a strictly convex regularisation function with the parameter $\lambda \geq 0$ tuning its strength.

State evolution equations. Let us now we present our main result, namely the exact asymptotic characterization of the distribution of the estimator $\mathbf{w}^* \in \mathbb{R}^d$ and of $\frac{1}{\sqrt{d}} \mathbf{w}^{*\top} \mathbf{X} \in \mathbb{R}^n$, where $\mathbf{X} \in \mathbb{R}^{d \times n}$ is the concatenation of the n dataset column vectors $\mathbf{x}^\nu \in \mathbb{R}^d$, $\nu \in [n]$. Such an asymptotic characterisation is performed via a set of order parameters satisfying a system of self-consistent ‘‘state-evolution’’ equations, that we will solve numerically. The asymptotic expressions for generalisation and training errors, in particular, can be written in terms of such order parameters. In the following, we use the shorthand $\ell_\pm(u) \equiv \ell(\pm 1, u)$. Also, given a function $\phi: \{-1, 1\} \rightarrow \mathbb{R}$, we will use the shorthand notation $\phi_\pm \equiv \phi(\pm 1)$ and denote $\mathbb{E}_\pm[\phi_\pm] = \rho_+ \phi_+ + \rho_- \phi_-$. We can now state the result.

Let $\zeta \sim \mathcal{N}(0, 1)$ and $\Delta \sim \varrho$, both independent from other quantities. Let also be $\xi \sim \mathcal{N}(\mathbf{0}, \mathbf{I}_d)$. Given $\phi_1: \mathbb{R}^d \rightarrow \mathbb{R}$ and $\phi_2: \mathbb{R}^n \rightarrow \mathbb{R}$, the estimator \mathbf{w}^* and the matrix $\mathbf{z}^* := \frac{1}{\sqrt{d}} \mathbf{w}^* \mathbf{X} \in \mathbb{R}^n$, they verify:

$$\phi_1(\mathbf{w}^*) \xrightarrow[n, d \rightarrow +\infty]{\text{P}} \mathbb{E}_\xi [\phi_1(\mathbf{g})], \quad \phi_2(\mathbf{z}^*) \xrightarrow[n, d \rightarrow +\infty]{\text{P}} \mathbb{E}_\zeta [\phi_2(\mathbf{h})], \quad (4)$$

where we have introduced the proximal for the loss:

$$h_\pm = \arg \min_u \left[\frac{(u - \omega_\pm)^2}{2\Delta v} + \ell_\pm(u) \right], \quad \omega_\pm := m_\pm + b + \sqrt{q\Delta}\zeta \quad (5)$$

and $\mathbf{h} \in \mathbb{R}^{2 \times n}$ is obtained by concatenating $\rho_+ n$ quantities h_+ with $\rho_- n$ quantities h_- . We have also introduced the proximal $\mathbf{g} \in \mathbb{R}^d$:

$$\mathbf{g} = \arg \min_{\mathbf{w}} \left(\hat{v} \frac{\|\mathbf{w}\|^2}{2} - \sqrt{d} \sum_{k=\pm} \hat{m}_k \mathbf{w}^\top \boldsymbol{\mu}_k - \sqrt{\hat{q}} \boldsymbol{\xi}^\top \mathbf{w} + \lambda r(\mathbf{w}) \right). \quad (6)$$

The collection of parameters $(b, q, m_\pm, v, \hat{q}, \hat{m}_\pm, \hat{v})$ appearing in the equations above is given by the fixed point solution of the following self-consistent equations:

$$\begin{cases} m_\pm = \frac{1}{\sqrt{d}} \mathbb{E}_\xi [\mathbf{g}^\top \boldsymbol{\mu}_\pm], \\ q = \frac{1}{d} \mathbb{E}_\xi [\|\mathbf{g}\|^2], \\ v = \frac{1}{d} \hat{q}^{-1/2} \mathbb{E}_\xi [\mathbf{g}^\top \boldsymbol{\xi}], \end{cases} \quad \begin{cases} \hat{q} = \alpha \mathbb{E}_{\pm, \zeta, \Delta} [\Delta f_\pm^2], \\ \hat{v} = -\alpha q^{-1/2} \mathbb{E}_{\pm, \Delta, \zeta} [\sqrt{\Delta} f_\pm \zeta], \\ \hat{m}_\pm = \alpha \rho_\pm \mathbb{E}_{\Delta, \xi} [f_\pm], \end{cases} \quad \begin{cases} f_\pm := \frac{h_\pm - \omega_\pm}{v\Delta}, \\ b = \mathbb{E}_{\pm, \Delta, \zeta} [h_\pm - m_\pm]. \end{cases} \quad (7)$$

As in the purely Gaussian case, the state evolution equations naturally split the dependence on the form of the loss function ℓ , which is relevant in the computation of h_\pm , and on the regularisation part r , entering in the computation of \mathbf{g} . In the most general setting, the solution requires the solution of two convex minimisation problems, consisting of the computation of the two proximals related to the loss and the regularisation respectively [36]. As a consequence of the result above, the training loss ϵ_ℓ , the training error ϵ_t , and the test (or generalisation) error ϵ_g are given by

$$\epsilon_\ell = \mathbb{E}_{\pm, \zeta, \Delta} [\ell_\pm(h_\pm)], \quad \epsilon_t = 1 - \mathbb{E}_{\pm, \zeta, \Delta} [\hat{y}_\pm(h_\pm)], \quad \epsilon_g = 1 - \mathbb{E}_{\pm, \xi, \Delta} [\hat{y}_\pm(\omega_\pm)]. \quad (8)$$

In particular, the generalisation (or test) error in the asymptotic regime is written in terms of the statistics of ω_\pm^* , having the form in Eq. (5) on the fixed-point values m_\pm^* , q^* and b^* ,

$$\epsilon_g = \mathbb{E}_{\pm, \Delta, \zeta} [\mathbb{I}(\varphi(\omega_\pm^*) \neq \pm 1)]. \quad (9)$$

The training error depends on the (fixed-point) statistics of the loss proximal as

$$\epsilon_t = \frac{1}{n} \sum_{v=1}^n \mathbb{I} \left(\varphi \left(\frac{\mathbf{w}^{*\top} \mathbf{x}^v}{\sqrt{d}} + b^* \right) \neq y^v \right) \xrightarrow[n/d=\alpha]{n \rightarrow +\infty} \mathbb{E}_{\pm, \Delta, \zeta} [\mathbb{I}(\varphi(h_\pm) \neq \pm 1)]. \quad (10)$$

The derivation of the results above is given in Appendix A and is obtained via the replica method. Moreover, explicit forms for specific choices of ℓ or r highly simplify the equations in special cases. A very special case, in particular, is presented below.

Quadratic loss with ridge regularisation. In the case of a quadratic loss, $\ell(y, x) = \frac{1}{2} (y - x)^2$, an explicit formula for the proximal h_\pm in Eq. (5) and for the proximal \mathbf{g} in Eq. (6) can be easily found. As a result, we can obtain explicit expressions for the corresponding set of state evolution equations which become particularly suitable for a fast numerical solution:

$$\begin{cases} m_\pm = \frac{\sum_{k=\pm} \hat{m}_k \boldsymbol{\mu}_k^\top \boldsymbol{\mu}_\pm}{\lambda + \hat{v}}, \\ q = \frac{\sum_{kk'} \hat{m}_k \hat{m}_{k'} \boldsymbol{\mu}_k^\top \boldsymbol{\mu}_{k'} + \hat{q}}{(\lambda + \hat{v})^2}, \\ v = \frac{1}{\lambda + \hat{v}}, \end{cases} \quad \begin{cases} \hat{q} = \alpha \mathbb{E}_\pm [(\pm 1 - m_\pm - b)^2] \mathbb{E}_\Delta \left[\frac{\Delta}{(1+v\Delta)^2} \right] + \alpha q \mathbb{E}_\Delta \left[\frac{\Delta^2}{(1+v\Delta)^2} \right], \\ \hat{v} = \alpha \mathbb{E}_\Delta \left[\frac{\Delta}{1+v\Delta} \right], \\ \hat{m}_\pm = \alpha \rho_\pm (\pm 1 - m_\pm - b) \mathbb{E}_\Delta \left[\frac{1}{1+v\Delta} \right]. \end{cases} \quad (11)$$

In the equations above $\sum_{kk'} \equiv \sum_{k=\pm, k'=\pm}$.

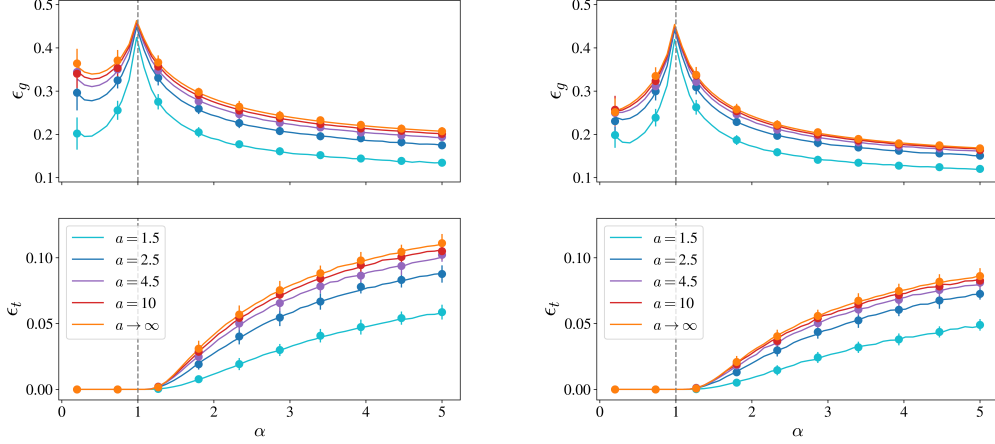


Figure 1: Test error ϵ_g (top) as predicted by Eq. (9) and training error ϵ_t (bottom) as predicted by Eq. (10) estimated by solving the fixed point equations (11) in the balanced $\rho = 1/2$ (left) and unbalanced $\rho = 1/4$ (right) case. The dataset distribution is parametrised as in Eq. (13), in both the balanced and unbalanced case. The classification task is solved using a quadratic loss with ridge regularisation with $\lambda = 10^{-5}$. Dots correspond to the average outcome of 50 numerical experiments in dimension $d = 10^3$. In our parametrisation, the population covariance is $\Sigma = \mathbf{I}_d$ for all values of a and moreover, for $a \rightarrow +\infty$, the case of pure Gaussian clouds $P(\mathbf{x}|\boldsymbol{\mu}) = \mathcal{N}(\mathbf{x}|\boldsymbol{\mu}, \mathbf{I}_d)$ is recovered. As expected, the interpolation peak is observed at $\alpha = 1$ for all values of a . Further details on the numerical solutions can be found in Appendix B.

3 Application to synthetic datasets

In this section, we compare our theoretical predictions with numerical results for a large family of data points distributions. We investigate in particular how well the asymptotic approximation captures the performance of the algorithm as we vary the parameters of the variance distribution ϱ , interpolating between power-law distributed points and Gaussian clouds. The results have been obtained using ridge ℓ_2 -regularisation, and both quadratic and logistic losses, with various data cluster balances ρ . We will omit the analysis of the simplest case $\varrho(\Delta) = \delta(\Delta - \Delta_0)$, which leads to a pair of Gaussian clouds with the same variance, a case discussed by Mignacco et al. [30]. In the following, we will assume, without loss of generality, that $\boldsymbol{\mu}_\pm = \pm \frac{1}{\sqrt{d}} \boldsymbol{\mu}$, where $\boldsymbol{\mu}$ is extracted from a distribution $\mathcal{N}(\mathbf{0}, \mathbf{I}_d)$. Our artificial data sets will be constructed using an inverse-Gamma distribution parameterised as

$$\varrho(\Delta) \equiv \varrho_{a,c}(\Delta) = \frac{c^a}{\Gamma(a)\Delta^{a+1}} e^{-\frac{c}{\Delta}}, \quad (12a)$$

depending on the shape parameter $a > 0$ and on the scale parameter $c > 0$, and leading to the following distribution of data points

$$P(\mathbf{x}|\boldsymbol{\mu}) = \frac{(2c)^a \Gamma(a + \frac{d}{2})}{\Gamma(a) \pi^{\frac{d}{2}}} (2c + \|\mathbf{x} - \boldsymbol{\mu}\|^2)^{-a - \frac{d}{2}}. \quad (12b)$$

This distribution has, for $a > 1$, covariance matrix $\Sigma = \mathbb{E}[(\mathbf{x} - \boldsymbol{\mu}) \otimes (\mathbf{x} - \boldsymbol{\mu})^\top] = \sigma^2 \mathbf{I}_d$, where $\sigma^2 = \frac{c}{a-1}$. For $a \in (0, 1]$, instead, $\sigma^2 = +\infty$. Note that the choice of inverse-Gamma distribution for ϱ is not that unusual. It has been adopted, for example, to describe non-Gaussian data in quantitative finance [7, 23] or econometrics models [32].

3.1 Finite covariance case

Let us start considering a data set distribution as in Eq. (12) with shape parameter $a = c + 1 > 1$. The data set distribution in this case is given by

$$P(\mathbf{x}|\boldsymbol{\mu}) = \frac{2^a (a-1)^a \Gamma(a + \frac{d}{2})}{\Gamma(a) \pi^{\frac{d}{2}}} (2a - 2 + \|\mathbf{x} - \boldsymbol{\mu}\|^2)^{-a - \frac{d}{2}} \quad (13)$$

and decays as $\|\mathbf{x}\|^{-2a-1}$ for $\|\mathbf{x} - \boldsymbol{\mu}\| \gg 0$, so that $\mathbb{E}[\|\mathbf{x} - \boldsymbol{\mu}\|^k] = +\infty$ for $k \geq 2a$. By this choice, all elements of the family in Eq. (13) have the same variance, $\sigma^2 = \mathbb{E}[\|\mathbf{x} - \boldsymbol{\mu}\|^2] = 1$, and, in the $a \rightarrow +\infty$ limit, $P(\mathbf{x}|\boldsymbol{\mu}) \rightarrow \mathcal{N}(\boldsymbol{\mu}, \mathbf{I}_d)$ recovering the pure Gaussian case. Note also that, in this case, the covariance matrix is given by $\boldsymbol{\Sigma} = \mathbb{E}[(\mathbf{x} - \boldsymbol{\mu}) \otimes (\mathbf{x} - \boldsymbol{\mu})^\top] = \mathbf{I}_d$ for all $a > 1$.

In Fig. 1 we present the results of our numerical experiments using the square loss and different regularisation strengths. An excellent agreement between the theoretical predictions and the results of numerical experiments is found for a range of values of a and sample complexity α , both for balanced, i.e., equally sized, and unbalanced clusters of data. The test error ϵ_g presents the classical interpolation peak at $\alpha = 1$, smoothed by the presence of a non-zero regularisation strength λ , and the typical double-descent behavior [33]. As a is increased, the results of Mignacco et al. [30] for Gaussian clouds with $P(\mathbf{x}|\boldsymbol{\mu}) = \mathcal{N}(\mathbf{x}|\boldsymbol{\mu}, \mathbf{I}_d)$ are recovered. The plot shows that, at given population covariance $\boldsymbol{\Sigma} = \mathbf{I}_d$, the classification of power-law distributed clouds has a different, and in particular smaller, test error than the corresponding task on Gaussian clouds with the same covariance. We interpret this as a heavy-tail effect: learning benefits from the presence of many data points which are far from their corresponding class means $\boldsymbol{\mu}_\pm$, although on average at finite distance σ . Moreover, test errors are systematically smaller for unbalanced clusters ($\rho = 1/4$) than for balanced clusters.

The same numerical experiment has been repeated using the logistic loss for training. Once again, in Fig. 2, we focus on $\rho = 1/2$ and show that the theoretical predictions of the generalisation and training errors agree with the results of numerical experiments for a range of sample complexity values α and various values of a , for both small and large regularisation.

Just as for the square loss, we observe in general that in the large limit for the parameter a for which the Gaussian case $P(\mathbf{x}|\boldsymbol{\mu}) = \mathcal{N}(\mathbf{x}|\boldsymbol{\mu}, \mathbf{I}_d)$ is recovered, the test error ϵ_g is larger than for power-law distributed clouds at finite values of a in Eq. (13). In the $\lambda \rightarrow 0$ limit, the typical interpolation cusp in the generalisation error for both the Gaussian and power-law distributed clouds is observed. A comparison with the test error ϵ_t confirms that this cusp occurs at the value of α where the training error becomes non-zero and the two training data clouds become non-separable [44, 8]. This sharp transition in α also corresponds to the existence transition of maximum-likelihood estimator in high-dimensional logistic regression for Gaussian data as shown by Sur and Candès [44]. For larger regularisation strength, the cusp smoothens, and the training error becomes non-zero at smaller values of the sample complexity α .

3.2 Infinite covariance case

The family of distributions specified by Eq. (12) allows us to also consider the case of infinite variance, $\sigma^2 = +\infty$. We interpolated in particular between the case of purely Gaussian clouds and the case of an infinite-variance point distribution using the general form in Eq. (12) with $c = 1$ and $a = 1/2$, by choosing $\varrho(\Delta) = r\varrho_{\frac{1}{2},1}(\Delta) + (1-r)\delta(\Delta-1)$. Each data point cloud has therefore infinite variance for $0 < r \leq 1$ and the Gaussian limit is recovered for $r = 0$. We solved the problem using both square loss and logistic loss, with a small ridge regularisation. Fig. 3 collects our results for two balanced clouds. A good agreement between the theoretical predictions and the results of numerical

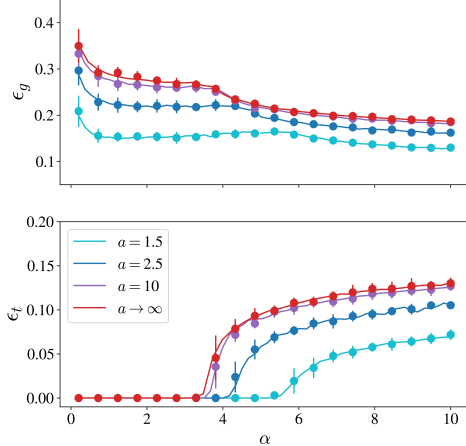


Figure 2: Test error ϵ_g (top) and training error ϵ_t (bottom) via logistic loss training on balanced clusters. The dataset distribution is parametrised as in Eq. (13). A ridge regularisation with $\lambda = 10^{-4}$ is adopted. Dots correspond to the average outcome of 20 numerical experiments in dimension $d = 10^3$. As in Fig. 1, the population covariance is here $\boldsymbol{\Sigma} = \mathbf{I}_d$, and the Gaussian limit is recovered for $a \rightarrow +\infty$. Further details on the numerical solutions can be found in Appendix B.

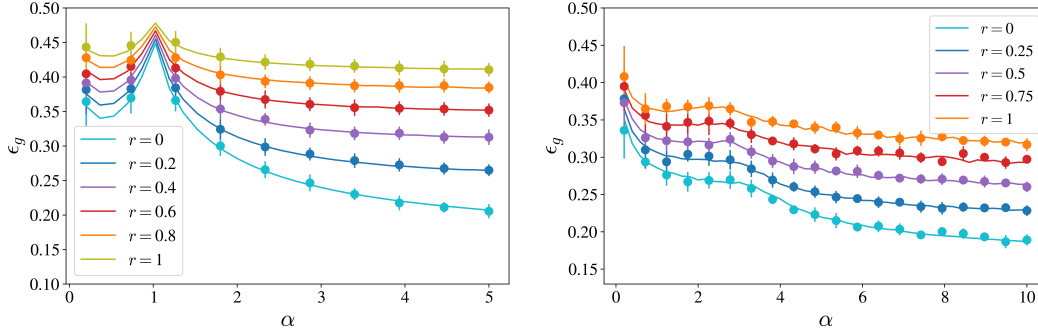


Figure 3: Test error ϵ_g in the classification of two balanced clouds via quadratic loss (**left**) and logistic loss (**right**). In both cases, ridge regularisation is adopted ($\lambda = 10^{-4}$ for the square loss case, $\lambda = 10^{-3}$ for the logistic loss case). Each cloud is a superposition of a power-law distribution with infinite variance and a Gaussian with covariance $\Sigma = \mathbf{I}_d$. The parameter r allows us to interpolate between the purely Gaussian limit ($r = 0$) and the infinite-variance limit ($0 < r \leq 1$). Dots correspond to the average test error of 20 numerical experiments in dimension $d = 10^3$. Note that, at a given sample complexity, Gaussian clouds are associated with the lowest test error for both losses.

experiments is found for a range of values of sample complexity and of the ratio r . Not surprisingly, the finite-variance case $r = 0$ corresponds to the lowest test error with both losses.

3.3 The role of regularisation in the classification of non-Gaussian clouds

One of the main results in the work of Mignacco et al. [30] on the classification of noisy Gaussian clouds is the effect of regularisation on the achievable performances. In particular, they observed that, for all values of the sample complexity α , the optimal ridge classification performance on a pair of balanced clouds is obtained for an infinite regularisation strength λ , using both hinge loss and square loss. Our framework allows testing the robustness of this result beyond the purely Gaussian setting. In Fig. 4 (left), we plot the test error obtained using the square loss and different regularisation strengths λ on the dataset distribution as in Eq. (13) at finite $a = 2$. We observe that, both in the balanced case and in the unbalanced case, the optimal regularisation strength λ^* is *finite* and, moreover, α -dependent. On the other hand, if we fix α and let a grow towards $+\infty$, the optimal λ^* grows as well to recover the result of Mignacco et al. [30] of diverging optimal regularisation for balanced Gaussian clouds, as shown in Fig. 4 (center). Therein, we fix $\alpha = 2$ and we extract, for each value of a , the value of λ^* that minimises the test error ϵ_g in the case of balanced clusters, showing that it is indeed finite for finite a and diverges as $a \rightarrow +\infty$, see Fig. 4 (right). Fig. 4 (right) also shows that, in the unbalanced case, the optimal regularisation strength λ^* saturates for $a \rightarrow +\infty$ to a finite value, as for Gaussian clouds [30].

3.4 The separability threshold

By studying the training error ϵ_t with logistic loss at zero regularisation we can obtain information on the boundary between the region in which the training data are perfectly separable and the regime in which they are not. In other words, we can extract the value of the so-called separability transition complexity α^* [44, 30, 25]. Once again, a complete characterisation of this transition point is available in the Gaussian case when $P(\mathbf{x}|\boldsymbol{\mu}) = \mathcal{N}(\mathbf{x}|\boldsymbol{\mu}, \sigma^2 \mathbf{I}_d)$ as a function of σ^2 [30]. It is however not trivial to extend such a result to non-Gaussian distributions and, in particular, to the case of distribution with infinite variance.

It is possible to estimate the position of the interpolation threshold α^* in the large family of “superstatistical” models via direct computation of ϵ_t for different values of α . Fig. 5, in particular, contains the values of α^* for different choices of the shape parameters a and c in the case of two balanced clouds of datapoints distributed as in Eq. (12b). The value is obtained by solving the state evolution equations in Eq. (7) with negligible ridge regularisation strength, and by recording the value of sample complexity a non-zero training error is produced. In Fig. 5 (left), we fixed the data variance $\sigma^2 = \mathbb{E}[\|\mathbf{x} - \boldsymbol{\mu}\|^2] = \frac{c}{a-1} < +\infty$, and plotted the separability threshold α^* for a range of

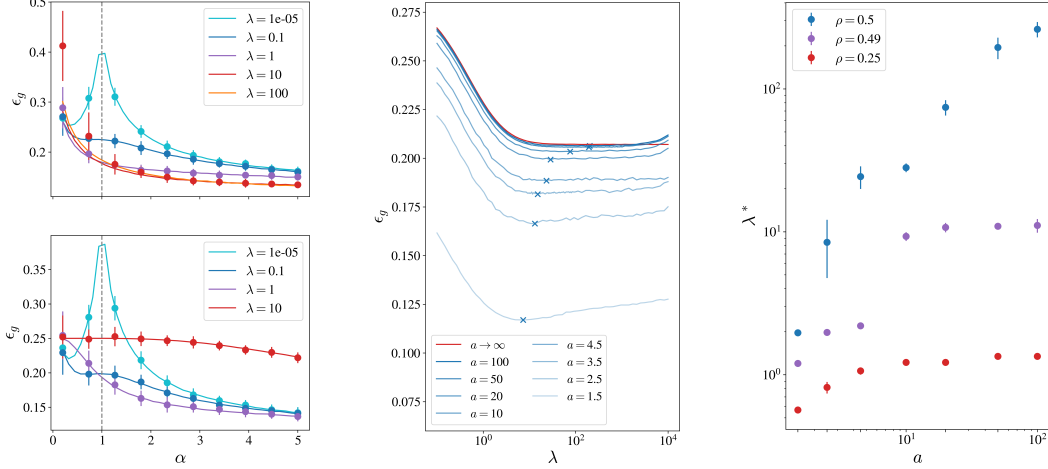


Figure 4: **(Left)** Test error for ridge regularised quadratic loss for various regularisation strengths. The data points of each cloud in the training set are distributed as in Eq. (13), with shape parameter $a = 2$, for balanced clusters (top) and unbalanced clusters ($\rho = 1/4$, bottom). Points are results of 50 numerical experiments. **(Center)** Test error for different regularisation strengths λ for two *balanced* clusters with quadratic loss at sample complexity $\alpha = 2$ using the data distribution (13). Note that $\sigma^2 = 1$ for all values of a . The optimal regularisation strength value λ^* for each a is marked with a cross. **(Right)** Optimal regularisation strength λ^* at $\alpha = 2$ for different values of $a \in [1.5, 10^2]$ for both balanced and unbalanced clusters. Note that, for $\rho = 1/2$, $\lambda^* \rightarrow +\infty$ as $a \rightarrow +\infty$.

values of the shape parameter $a > 1$. As a grows at fixed σ^2 , the distribution Eq. (13) converges to a Gaussian distribution $\mathcal{N}(\mu, \sigma^2 \mathbf{I}_d)$, and therefore α^* approaches the threshold value of the Gaussian case found by Mignacco et al. [30]. By taking the double limit $a \rightarrow \infty$ and $\sigma^2 \rightarrow \infty$, on the other hand, the Cover [5] transition value $\alpha^* = 2$ is recovered, as expected. In Fig. 5 (right), instead, we analyse the case of infinite-variance clusters, by choosing $0 < a < 1$ and varying the scale parameter c in the data distribution Eq. (12b). It is clear that, in this setting, we have no variance as a “scale reference”, and c plays the role of distribution width. The Cover transition is therefore correctly recovered as c diverges for all values of a .

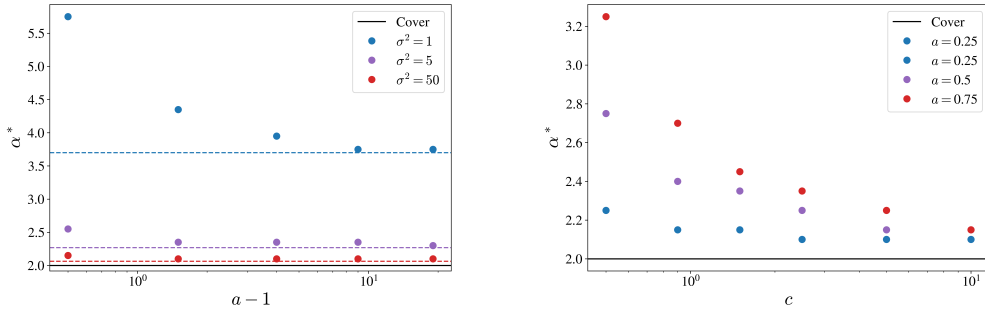


Figure 5: Separability threshold α^* obtained by solving the equations in Eq. (7) with logistic loss, ridge regularisation strength $\lambda = 10^{-5}$ and $\rho = 1/2$. The data points of each cloud are distributed around their mean μ with a two-parameter distribution as in Eq. (12b). **(Left)** Finite covariance $\Sigma = \sigma^2 \mathbf{I}_d$ case, $\sigma^2 = \frac{c}{a-1}$, as a function of a . Dashed lines are the threshold values of the Gaussian case [30]. At large a and large variance σ^2 , the Cover’s transition $\alpha = 2$ for balanced clusters (black line) is recovered. **(Right)** Infinite-variance data clusters case. The cluster distribution is obtained by fixing $0 < a < 1$ in Eq. (12b). As the scale parameter c grows, the threshold value approaches Cover’s transition $\alpha = 2$ for balanced clusters (black line).

Acknowledgements

The authors would like to thank Nikolas Nüsken for stimulating discussions. Also, we would like to thank Bruno Loureiro for his feedbacks and for his careful reading of the manuscript.

References

- [1] C. Beck. Superstatistics: Theory and applications. *Contin. Mech. Thermodyn.*, 16, 03 2003.
- [2] C. Beck and E.G.D. Cohen. Superstatistics. *Physica A*, 322:267–275, 2003.
- [3] M. Belkin, D. Hsu, S. Ma, and S. Mandal. Reconciling modern machine-learning practice and the classical bias–variance trade-off. *Proc. Natl. Acad. Sci. U.S.A.*, 116(32):15849–15854, 2019.
- [4] M. Belkin, A. Rakhlin, and A.B. Tsybakov. Does data interpolation contradict statistical optimality? In K. Chaudhuri and M. Sugiyama, editors, *Proceedings of the 22nd International Conference on Artificial Intelligence and Statistics*, volume 89 of *Proc. Mach. Learn. Res.*, pages 1611–1619. PMLR, 2019.
- [5] T.M. Cover. Geometrical and statistical properties of systems of linear inequalities with applications in pattern recognition. *IEEE Trans. Comput.*, EC-14(3):326–334, 1965.
- [6] P. del Giudice, S. Franz, and M. Virasoro. Perceptron beyond the limit of capacity. *J. Physique*, 50:121–134, 01 1989.
- [7] D. Delpini and G. Bormetti. Minimal model of financial stylized facts. *Phys. Rev. E*, 83:041111, 2011.
- [8] A. Deng, Z. Kammoun and C. Thrampoulidis. A model of double descent for high-dimensional binary linear classification. *Inf. Inference*, 11, 2021.
- [9] N. El Karoui. On the impact of predictor geometry on the performance on high-dimensional ridge-regularized generalized robust regression estimators. *Probab. Theory Relat. Fields*, 170, 2018.
- [10] S. Franz, D.J. Amit, and M.A. Virasoro. Prosopagnosia in high capacity neural networks storing uncorrelated classes. *J. Physique*, 51(5):387–408, 1990.
- [11] E Gardner. The space of interactions in neural network models. *J. Phys. A: Math. Gen.*, 21(1): 257, 1988.
- [12] E. Gardner and B. Derrida. Three unfinished works on the optimal storage capacity of networks. *J. Phys. A: Math. Gen.*, 22(12):1983, 1989.
- [13] F. Gerace, B. Loureiro, F. Krzakala, M. Mézard, and L. Zdeborová. Generalisation error in learning with random features and the hidden manifold model. In *ICML*, pages 3452–3462, 2020.
- [14] F. Gerace, F. Krzakala, B. Loureiro, L. Stephan, and L. Zdeborová. Gaussian universality of perceptrons with random labels. *arXiv:2205.13303*, 2022.
- [15] B. Ghorbani, S. Mei, T. Misiakiewicz, and A. Montanari. Limitations of lazy training of two-layers neural network. In H. Wallach, H. Larochelle, A. Beygelzimer, F. d'Alché-Buc, E. Fox, and R. Garnett, editors, *Advances in Neural Information Processing Systems*, volume 32, 2019.
- [16] S. Goldt, M. Mézard, F. Krzakala, and L. Zdeborová. Modeling the influence of data structure on learning in neural networks: The hidden manifold model. *Phys. Rev. X*, 10:041044, Dec 2020.
- [17] S. Goldt, M. Mézard, F. Krzakala, and L. Zdeborová. Modeling the influence of data structure on learning in neural networks: The hidden manifold model. *Phys. Rev. X*, 10:041044, 2020.
- [18] T. Hastie, R. Tibshirani, and J.H. Friedman. *The elements of statistical learning: data mining, inference, and prediction*, volume 2. Springer, 2009.

- [19] T. Hastie, A. Montanari, S. Rosset, and R.J. Tibshirani. Surprises in high-dimensional ridgeless least squares interpolation. *Ann. Stat.*, 50(2):949 – 986, 2022.
- [20] G.R. Kini and C. Thrampoulidis. Phase transitions for one-vs-one and one-vs-all linear separability in multiclass gaussian mixtures. In *ICASSP 2021*, pages 4020–4024, 2021.
- [21] V. Kothapalli, E. Rasromani, and V. Awatramani. Neural collapse: A review on modelling principles and generalization. *arXiv:2206.04041*, 2022.
- [22] W. Krauth and M. Mézard. Storage capacity of memory networks with binary couplings. *J. Physique*, 50(20):3057–3066, 1989.
- [23] Nicolas Langrené, Geoffrey Lee, and Zili Zhu. Switching to non-affine stochastic volatility: A closed-form expansion for the inverse gamma model. *Int. J. Theor. Appl. Finance*, 19, 2015.
- [24] M. Lelarge and L. Miolane. Asymptotic bayes risk for gaussian mixture in a semi-supervised setting. In *2019 IEEE 8th International Workshop on Computational Advances in Multi-Sensor Adaptive Processing*, pages 639–643, 2019.
- [25] B. Loureiro, G. Sicuro, C. Gerbelot, A. Pacco, F. Krzakala, and L. Zdeborová. Learning Gaussian Mixtures with Generalized Linear Models: Precise Asymptotics in High-dimensions. *Advances in Neural Information Processing Systems*, 34:10144–10157, 2021.
- [26] B. Loureiro, C. Gerbelot, H. Cui, S. Goldt, F. Krzakala, M. Mézard, and L. Zdeborová. Learning curves of generic features maps for realistic datasets with a teacher-student model. *J. Stat. Mech.: Theory Exp.*, 2022(11):114001, 2022.
- [27] X. Mai and Z. Liao. High dimensional classification via regularized and unregularized empirical risk minimization: Precise error and optimal loss. *arXiv:1905.13742*, 2020.
- [28] S. Mei and A. Montanari. The Generalization Error of Random Features Regression: Precise Asymptotics and the Double Descent Curve. *Commun. Pure Appl. Math.*, 75, 2019.
- [29] M. Mézard, G. Parisi, and M.A. Virasoro. *Spin glass theory and beyond: An Introduction to the Replica Method and Its Applications*, volume 9. World Scientific Publishing Company, 1987.
- [30] F. Mignacco, F. Krzakala, Y. Lu, P. Urbani, and L. Zdeborová. The role of regularization in classification of high-dimensional noisy Gaussian mixture. In Hal Daumé III and Aarti Singh, editors, *Proceedings of the 37th International Conference on Machine Learning*, volume 119 of *Proc. Mach. Learn. Res.*, pages 6874–6883. PMLR, 13–18 Jul 2020.
- [31] A. Montanari and P.-M. Nguyen. Universality of the elastic net error. In *2017 IEEE ISIT*, pages 2338–2342. IEEE, 2017.
- [32] Daniel B Nelson. Arch models as diffusion approximations. *J. Econom.*, 45(1-2):7–38, 1990.
- [33] M. Opper, W. Kinzel, J. Kleinz, and R. Nehl. On the ability of the optimal perceptron to generalise. *J. Phys. A: Math. Gen.*, 23(11):L581, jun 1990.
- [34] A. Panahi and B. Hassibi. A universal analysis of large-scale regularized least squares solutions. In I. Guyon, U. Von Luxburg, S. Bengio, H. Wallach, R. Fergus, S. Vishwanathan, and R. Garnett, editors, *Advances in Neural Information Processing Systems*, volume 30. Curran Associates, Inc., 2017.
- [35] V. Pappayan, X.Y. Han, and D.L. Donoho. Prevalence of neural collapse during the terminal phase of deep learning training. *Proc. Natl. Acad. Sci. U.S.A.*, 117(40):24652–24663, 2020.
- [36] N. Parikh and S. Boyd. Proximal algorithms. *Found. Trends Optim.*, 1(3):127–239, jan 2014.
- [37] F. Pedregosa, G. Varoquaux, A. Gramfort, V. Michel, B. Thirion, O. Grisel, M. Blondel, P. Prettenhofer, R. Weiss, V. Dubourg, J. Vanderplas, A. Passos, D. Cournapeau, M. Brucher, M. Perrot, and E. Duchesnay. Scikit-learn: Machine learning in Python. *J. Mach. Learn. Res.*, 12:2825–2830, 2011.

- [38] L. Pesce, F. Krzakala, B. Loureiro, and L. Stephan. Are Gaussian data all you need? Extents and limits of universality in high-dimensional generalized linear estimation. *arXiv:2302.08923*, 2023.
- [39] A. Rahimi and B. Recht. Random features for large-scale kernel machines. In J. Platt, D. Koller, Y. Singer, and S. Roweis, editors, *Advances in Neural Information Processing Systems*, volume 20. Curran Associates, Inc., 2007.
- [40] S. Rosset, J. Zhu, and T. Hastie. Margin maximizing loss functions. In S. Thrun, L. Saul, and B. Schölkopf, editors, *Advances in Neural Information Processing Systems*, volume 16. MIT Press, 2003.
- [41] M.E.A. Seddik, C. Louart, M. Tamaazousti, and R. Couillet. Random matrix theory proves that deep learning representations of GAN-data behave as Gaussian mixtures. In H.D. III and A. Singh, editors, *Proceedings of the 37th International Conference on Machine Learning*, volume 119 of *Proc. Mach. Learn. Res.*, pages 8573–8582. PMLR, 13–18 Jul 2020.
- [42] H. S. Seung, H. Sompolinsky, and N. Tishby. Statistical mechanics of learning from examples. *Phys. Rev. A*, 45:6056–6091, 1992.
- [43] L. Steinberger and H. Leeb. Conditional predictive inference for stable algorithms.
- [44] P. Sur and E.J. Candès. A modern maximum-likelihood theory for high-dimensional logistic regression. *Proc. Natl. Acad. Sci. U.S.A.*, 116(29):14516–14525, 2019.
- [45] C. Thrampoulidis, E. Abbasi, and B. Hassibi. Precise error analysis of regularized m -estimators in high dimensions. *IEEE Trans. Inf. Theory*, 64(8):5592–5628, 2018.
- [46] C. Tsallis. Possible generalization of Boltzmann-Gibbs statistics. *Journal of Statistical Physics*, 52(1-2):479–487, 1988.
- [47] T.L.H. Watkin, A. Rau, and M. Biehl. The statistical mechanics of learning a rule. *Rev. Mod. Phys.*, 65:499–556, 1993.
- [48] Q. Zhao, P. Sur, and E.J. Candès. The asymptotic distribution of the MLE in high-dimensional logistic models: Arbitrary covariance. *Bernoulli*, 28(3):1835 – 1861, 2022.

A The replica approach

In this Appendix, we will derive the fixed point equations for the order parameters following the analysis by [25], and assuming that we deal with the classification of two clusters. The dataset $\mathcal{D} := \{(\mathbf{x}^y, y^y)\}_{y \in [n]}$ consists of n independent datapoints $\mathbf{x}^y \in \mathbb{R}^d$ each associated to a label $y^y \in \{-1, 1\}$. The elements of the dataset are independently generated by using a law $P(\mathbf{x}, y)$ which we assume can be put in the form $P(\mathbf{x}, y) \equiv \int_0^\infty P(\mathbf{x}, y|\Delta)\varrho(\Delta)d\Delta$ for some given distribution on the positive real axis ϱ , and such that

$$P(\mathbf{x}, y|\Delta) = \delta_{y,+1}\rho\mathcal{N}(\mathbf{x}|\boldsymbol{\mu}_+, \Delta\mathbf{I}_d) + \delta_{y,-1}(1-\rho)\mathcal{N}(\mathbf{x}|\boldsymbol{\mu}_-, \Delta\mathbf{I}_d), \quad \rho \in (0, 1). \quad (14)$$

The vectors $\boldsymbol{\mu}_\pm \in \mathbb{R}^d$ play the role of centroids of two clusters labeled by $y = +1$ and $y = -1$, respectively. We will perform our classification task searching for a set of parameters (\mathbf{w}^*, b^*) , called respectively *weights* and *bias*, that will allow us to construct an estimator via a certain classifier $\varphi: \mathbb{R} \rightarrow \{-1, 1\}$:

$$\mathbf{x} \mapsto \varphi\left(\frac{\mathbf{w}^* \top \mathbf{x}}{\sqrt{d}} + b^*\right), \quad (15)$$

which will provide us with our prediction for a datapoint \mathbf{x} . It is common to adopt $\varphi(x) = \text{sign}(x)$. The parameters will be chosen by minimising an empirical risk function in the form

$$\mathcal{R}(\mathbf{w}, b) \equiv \sum_{y=1}^n \ell\left(y^y, \frac{\mathbf{w} \top \mathbf{x}^y}{\sqrt{d}} + b\right) + \lambda r(\mathbf{w}), \quad (16)$$

i.e., they are given by

$$(\mathbf{w}^*, b^*) \equiv \arg \min_{\substack{\mathbf{w} \in \mathbb{R}^d \\ b \in \mathbb{R}}} \mathcal{R}(\mathbf{w}, b). \quad (17)$$

We will assume that ℓ is a convex loss function with respect to its second argument, and r is a regularisation function: the parameter $\lambda \geq 0$ will tune the strength of the regularisation. The starting point is to reformulate the problem as an optimisation problem by introducing a Gibbs measure over the parameters (\mathbf{w}, b) depending on a positive parameter β ,

$$\mu_\beta(\mathbf{w}, b) \propto e^{-\beta\mathcal{R}(\mathbf{w}, b)} = \underbrace{e^{-\beta r(\mathbf{w})}}_{P_w(\mathbf{w})} \prod_{y=1}^n \underbrace{\exp\left[-\beta\ell\left(y^y, \frac{\mathbf{w} \top \mathbf{x}^y}{\sqrt{d}} + b\right)\right]}_{P_y(y|\mathbf{w}, b)}, \quad (18)$$

so that, in the $\beta \rightarrow +\infty$ limit, the Gibbs measure concentrates on the values (\mathbf{w}^*, b^*) which minimize the empirical risk $\mathcal{R}(\mathbf{w}, b)$ and are therefore the goal of the learning process. The functions P_y and P_w can be interpreted as (unnormalised) likelihood and prior distribution respectively. Our analysis will go through the computation of the average free energy density associated with such Gibbs measure in a specific proportional limit, i.e.,

$$f_\beta = - \lim_{\substack{n, d \rightarrow +\infty \\ n/d = \alpha}} \mathbb{E}_{\mathcal{D}} \left[\frac{\ln \mathcal{Z}_\beta}{d\beta} \right], \quad (19)$$

where $\mathbb{E}_{\mathcal{D}}[\bullet]$ is the average over the training dataset, and we have introduced the partition function

$$\mathcal{Z}_\beta \equiv \int e^{-\beta\mathcal{R}(\mathbf{w}, b)} d\mathbf{w}. \quad (20)$$

To perform the computation of such quantity, we use the so-called replica method, i.e., we compute

$$- \lim_{\substack{n, d \rightarrow +\infty \\ n/d = \alpha}} \mathbb{E}_{\mathcal{D}} \left[\frac{\ln \mathcal{Z}_\beta}{d\beta} \right] = \lim_{\substack{n, d \rightarrow +\infty \\ n/d = \alpha}} \lim_{s \rightarrow 0} \frac{1 - \mathbb{E}_{\mathcal{D}}[\mathcal{Z}_\beta^s]}{sd\beta}. \quad (21)$$

A.1 Replica approach

We proceed in our calculation by considering the bias vector assuming no prior on b , which will play a role of an extra parameter. The equations for the low-dimensional bias b will be derived extremising with respect to it the final result for the free energy. We need to evaluate

$$\mathbb{E}_{\mathcal{D}}[\mathcal{Z}_\beta^s] = \prod_{a=1}^s \int d\mathbf{w}^a P_w(\mathbf{w}^a) \left(\sum_{k=\pm} \rho_k \mathbb{E}_{\mathbf{x}^k} \left[\prod_{a=1}^s P_k\left(\frac{\mathbf{w}^a \top \mathbf{x}}{\sqrt{d}} + b\right) \right] \right)^n. \quad (22)$$

Here and in the following $\rho \equiv \rho_+ = 1 - \rho_-$ and $P_\pm(\eta) \equiv P_y(\pm 1|\eta)$. Let us take the inner average introducing a new set of variables η^a ,

$$\begin{aligned} \mathbb{E}_{\mathbf{x}|k} \left[\prod_{a=1}^s P_k \left(\frac{\mathbf{w}^{a\top} \mathbf{x}}{\sqrt{d}} + b \right) \right] &= \prod_{a=1}^s \int d\eta^a P_k(\eta^a) \mathbb{E}_{\mathbf{x}|k} \left[\prod_{a=1}^s \delta \left(\eta^a - \frac{\mathbf{w}^{a\top} \mathbf{x}}{\sqrt{d}} + b \right) \right] \\ &= \mathbb{E}_{\Delta|k} \left[\prod_{a=1}^s \int d\eta^a P_k(\eta^a) \mathcal{N} \left(\boldsymbol{\eta} \middle| \frac{\mathbf{w}^{a\top} \boldsymbol{\mu}_k}{\sqrt{d}} - b; \frac{\Delta \mathbf{w}^a \mathbf{w}^{b\top}}{d} \right) \right], \end{aligned} \quad (23)$$

where we used the superstatistical form of the distribution of a datapoint \mathbf{x} . Using the shorthand $\mathbb{E}_{k,\Delta}[f_k(\Delta)] \equiv \sum_{k=\pm} \rho_k \int_0^\infty \varrho(\Delta) f_k(\Delta) d\Delta$, we can write then

$$\begin{aligned} \mathbb{E}_{\mathcal{D}}[\mathcal{Z}_\beta^s] &= \prod_{a=1}^s \int d\mathbf{w}^a P_w(\mathbf{w}^a) \left(\mathbb{E}_{k,\Delta} \left[\prod_{a=1}^s \int d\eta^a P_k(\eta^a) \mathcal{N} \left(\boldsymbol{\eta}; \frac{\mathbf{w}^{a\top} \boldsymbol{\mu}_k}{d} + b; \frac{\Delta \mathbf{w}^a \mathbf{w}^{b\top}}{d} \right) \right] \right)^n \\ &= \left(\prod_{a \leq b} \iint \mathcal{D}Q^{ab} \mathcal{D}\hat{Q}^{ab} \right) \left(\prod_a \mathcal{D}m^a \mathcal{D}\hat{m}^a \right) e^{-d\beta\Phi^{(s)}}. \end{aligned} \quad (24)$$

In the equation above we introduced the *order parameters*

$$Q_\Delta^{ab} = \Delta \frac{\mathbf{w}^{a\top} \mathbf{w}^b}{d} \in \mathbb{R}, \quad a, b = 1, \dots, s, \quad (25)$$

$$m_k^a = \frac{\mathbf{w}^{a\top} \boldsymbol{\mu}_k}{\sqrt{d}} \in \mathbb{R}, \quad a = 1, \dots, s, \quad (26)$$

whilst $\iint \mathcal{D}Q^{ab} \mathcal{D}\hat{Q}^{ab}$ express the integration over all possible functions of ΔQ_Δ^{ab} and \hat{Q}_Δ^{ab} . Similarly, $\mathcal{D}m^a \mathcal{D}\hat{m}^a \propto \prod_{k=\pm} dm_k^a d\hat{m}_k^a$. In the equation, we have also denoted the replicated free-energy

$$\begin{aligned} \beta\Phi^{(s)}(Q, M, \hat{Q}, \hat{m}, b) &= \sum_{k=\pm} \sum_a \hat{m}_k^{a\top} m_k^a + \sum_{a \leq b} \mathbb{E}_\Delta[\hat{Q}_\Delta^{ab} Q_\Delta^{ab}] \\ &\quad - \frac{1}{d} \ln \prod_{a=1}^s \int P_w(\mathbf{w}^a) d\mathbf{w}^a \left(\prod_{a \leq b} e^{\mathbb{E}_\Delta[\Delta \hat{Q}_\Delta^{ab}] \mathbf{w}^{a\top} \mathbf{w}^b} \prod_a e^{\sqrt{d} \sum_k \hat{m}_k^a \mathbf{w}^{a\top} \boldsymbol{\mu}_k} \right) \\ &\quad - \alpha \ln \mathbb{E}_{k,\Delta} \left[\prod_{a=1}^s \int d\eta^a P_k(\eta^a) \mathcal{N} \left(\boldsymbol{\eta} \middle| m_k^a + b, Q_\Delta^{ab} \right) \right]. \end{aligned} \quad (27)$$

At this point, the free energy f_β should be computed functionally extremizing with respect to all the order parameters by virtue of the Laplace approximation (in addition to b),

$$f_\beta = \lim_{s \rightarrow 0} \text{Extr}_{\substack{m, \hat{m} \\ Q, \hat{Q}, b}} \frac{\Phi^{(s)}(Q, m, \hat{Q}, \hat{m}, b)}{s}. \quad (28)$$

However, the convexity of the problem allows us to make an important simplification.

Replica symmetric ansatz — Before taking the $s \rightarrow 0$ limit we make the replica symmetric assumptions

$$\begin{aligned} Q_\Delta^{aa} &= \begin{cases} R_\Delta, & a = b \\ Q_\Delta, & a \neq b \end{cases} & \hat{Q}_\Delta^{aa} &= \begin{cases} -\frac{1}{2} \hat{R}_\Delta, & a = b \\ \hat{Q}_\Delta, & a \neq b \end{cases} \\ m_k^a &= m_k & \hat{m}_k^a &= \hat{m}_k \quad \forall a \end{aligned} \quad (29)$$

By means of the replica symmetric hypothesis, we can write

$$Q_\Delta^{ab} \mapsto \mathbf{Q}_\Delta \equiv (R_\Delta - Q_\Delta) \mathbf{I}_{s,s} + Q_\Delta \mathbf{1}_s. \quad (30)$$

The inverse matrix is therefore

$$\mathbf{Q}_\Delta^{-1} = \frac{1}{R_\Delta - Q_\Delta} \mathbf{1}_s - \frac{Q_\Delta}{(R_\Delta - Q_\Delta + sQ_\Delta)(R_\Delta - Q_\Delta)} \mathbf{I}_{s,s}, \quad (31)$$

whereas

$$\det \mathbf{Q}_\Delta = (R_\Delta - Q_\Delta)^{s-1} (R_\Delta - Q_\Delta + sQ_\Delta) = 1 + s \ln(R_\Delta - Q_\Delta) + s \frac{Q_\Delta}{R_\Delta - Q_\Delta} + o(s). \quad (32)$$

If we denote $V_\Delta := R_\Delta - Q_\Delta$

$$\ln \mathbb{E}_{k,\Delta} \left[\prod_{a=1}^s \int d\eta^a P_k(\eta^a) \mathcal{N}(\boldsymbol{\eta} | m_k^a + b, Q_\Delta^{ab}) \right] = s \mathbb{E}_{k,\Delta,\xi} \left[\ln Z_k(m_k + b + \sqrt{Q_\Delta} \xi, V_\Delta) \right] + o(s), \quad (33)$$

with $\xi \sim \mathcal{N}(0, 1)$ is normally distributed and we have introduced the function

$$Z_k(m, V) \equiv \int \frac{d\eta P_k(\eta)}{\sqrt{2\pi V}} e^{-\frac{(\eta-m)^2}{2V}}. \quad (34)$$

On the other hand, denoted by $\hat{V}_\Delta = \hat{R}_\Delta + \hat{Q}_\Delta$,

$$\begin{aligned} & \frac{1}{d} \ln \prod_{a=1}^s \left(\int P_w(\mathbf{w}^a) d\mathbf{w}^a e^{-\mathbb{E}_\Delta[\Delta \hat{V}_\Delta] \frac{\|\mathbf{w}^a\|^2}{2} + \sqrt{d} \sum_k \hat{m}_k \mathbf{w}^{a\top} \boldsymbol{\mu}_k} \prod_b e^{\frac{1}{2} \mathbb{E}_\Delta[\Delta \hat{Q}_\Delta] \mathbf{w}^{a\top} \mathbf{w}^b} \right) = \\ & = \frac{s}{d} \mathbb{E}_\xi \ln \left[\int P_w(\mathbf{w}) d\mathbf{w} \exp \left(-\mathbb{E}_\Delta[\Delta \hat{V}_\Delta] \frac{\|\mathbf{w}\|^2}{2} + \sqrt{d} \sum_k \hat{m}_k \mathbf{w}^\top \boldsymbol{\mu}_k + \sqrt{\mathbb{E}_\Delta[\Delta \hat{Q}_\Delta]} \boldsymbol{\xi}^\top \mathbf{w} \right) \right] + o(s). \end{aligned} \quad (35)$$

In the expression above we have introduced $\boldsymbol{\xi} \in \mathbb{R}^d$ having i.i.d. random Gaussian entries with zero mean and variance 1, and the average over them $\mathbb{E}_\xi[\bullet]$. Therefore, the (replicated) *replica symmetric* free-energy is given by

$$\lim_{s \rightarrow 0} \frac{\beta}{s} \Phi_{\text{RS}}^{(s)} = \sum_{k=1}^K \hat{m}_k m_k + \frac{\mathbb{E}_\Delta[\hat{V}_\Delta Q_\Delta - \hat{Q}_\Delta V_\Delta - \hat{V}_\Delta V_\Delta]}{2} - \alpha \beta \Psi_{\text{out}}(m, Q, V) - \beta \Psi_w(\hat{m}, \hat{Q}, \hat{V}) \quad (36)$$

where we have defined two contributions

$$\begin{aligned} \Psi_{\text{out}}(m, Q, V) & \equiv \beta^{-1} \mathbb{E}_{k,\Delta,\xi} [\ln Z_k(\omega_k, V_\Delta)] \\ \Psi_w(\hat{m}, \hat{Q}, \hat{V}) & \equiv \frac{1}{\beta d} \mathbb{E}_\xi \ln \left[\int P_w(\mathbf{w}) d\mathbf{w} \exp \left(-\mathbb{E}_\Delta[\Delta \hat{V}_\Delta] \frac{\|\mathbf{w}\|^2}{2} + \sqrt{d} \sum_k \hat{m}_k \mathbf{w}^\top \boldsymbol{\mu}_k + \sqrt{\mathbb{E}_\Delta[\Delta \hat{Q}_\Delta]} \boldsymbol{\xi}^\top \mathbf{w} \right) \right] \end{aligned} \quad (37)$$

and introduced, for future convenience,

$$\omega_k := m_k + b + \sqrt{Q_\Delta} \xi. \quad (38)$$

Note that we have separated the contribution coming from the chosen loss (the so-called *channel* part Ψ_{out}) from the contribution depending on the regularisation (the *prior* part Ψ_w). To write down the saddle-point equations in the $\beta \rightarrow +\infty$ limit, let us first rescale our order parameters as $\hat{m}_k \mapsto \beta \hat{m}_k$, $\hat{Q}_\Delta \mapsto \beta^2 \hat{Q}_\Delta$, $\hat{V} \mapsto \beta \hat{V}$ and $V_\Delta \mapsto \beta^{-1} V_\Delta$. For $\beta \rightarrow +\infty$ the channel part is

$$\Psi_{\text{out}}(m, Q, V) = -\mathbb{E}_{k,\Delta,\xi} \left[\frac{(h_k - \omega_k)^2}{2V_\Delta} + \ell_k(h_k) \right]. \quad (39)$$

where we have written Ψ_{out} in terms of a proximal

$$\arg \min_u \left[\frac{(u - \omega_k)^2}{2V_\Delta} + \ell_k(u) \right]. \quad (40)$$

A similar expression can be obtained for Ψ_w . Introducing the proximal

$$\mathbf{g} = \arg \min_{\mathbf{w}} \left(\frac{\mathbb{E}_\Delta[\Delta \hat{V}_\Delta] \|\mathbf{w}\|^2}{2} - \sqrt{d} \sum_k \hat{m}_k \mathbf{w}^\top \boldsymbol{\mu}_k - \sqrt{\mathbb{E}_\Delta[\Delta \hat{Q}_\Delta]} \boldsymbol{\xi}^\top \mathbf{w} + \lambda r(\mathbf{w}) \right) \in \mathbb{R}^d \quad (41)$$

We can rewrite the prior contribution Ψ_w as

$$\Psi_w(\hat{m}, \hat{Q}, \hat{V}) = -\frac{1}{d} \mathbb{E}_\xi \left[\frac{\mathbb{E}_\Delta[\Delta \hat{V}_\Delta] \|\mathbf{g}\|^2}{2} - \sqrt{d} \sum_k \hat{m}_k \mathbf{g}^\top \boldsymbol{\mu}_k - \sqrt{\mathbb{E}_\Delta[\Delta \hat{Q}_\Delta]} \boldsymbol{\xi}^\top \mathbf{g} + \lambda r(\mathbf{g}) \right] \quad (42)$$

The parallelism between the two contributions is evident, aside from the different dimensionality of the involved objects. The replica symmetric free energy in the $\beta \rightarrow +\infty$ limit is computed extremising with respect to the introduced order parameters,

$$f_{\text{RS}} = \text{Extr}_{\substack{M, Q, V, b \\ \hat{m}, \hat{Q}, \hat{V}}} \left[\sum_{k=\pm} \hat{m}_k m_k + \frac{\mathbb{E}_{\Delta} [\hat{V}_{\Delta} Q_{\Delta} - \hat{Q}_{\Delta} V_{\Delta} - \hat{V}_{\Delta} V_{\Delta}]}{2} - \alpha \Psi_{\text{out}}(m, Q, V) - \Psi_w(\hat{m}, \hat{Q}, \hat{V}) \right]. \quad (43)$$

To do so, we have to write down a set of saddle-point equations and solve them.

Saddle-point equations — The saddle-point equations are derived straightforwardly from the obtained free energy functionally extremising with respect to all parameters. A first set of equations is obtained from Ψ_{out} . Introducing

$$f_k \equiv \frac{h_k - \omega_k}{V_{\Delta}}. \quad (44)$$

(and keeping in mind that this quantity is also Δ -dependent) we have

$$\hat{Q}_{\Delta} = \alpha \mathbb{E}_{k, \xi} [f_k^2], \quad \hat{V}_{\Delta} = -\frac{\alpha \mathbb{E}_{k, \xi} [f_k \xi]}{\sqrt{Q_{\Delta}}}, \quad \hat{m}_k = \alpha \rho_k \mathbb{E}_{\Delta, \xi} [f_k], \quad b = \mathbb{E}_{k, \Delta, \xi} [h_k - m_k]. \quad (45)$$

Denoting $\hat{q} := \mathbb{E}[\Delta \hat{Q}_{\Delta}]$ and $\hat{v} := \mathbb{E}[\Delta \hat{V}_{\Delta}]$, the saddle-point equations from Ψ_w are

$$V_{\Delta} = \frac{1}{d} \frac{\Delta \mathbb{E}_{\xi} [\mathbf{g}^{\top} \xi]}{\sqrt{\hat{q}}} \quad Q_{\Delta} = \frac{\Delta}{d} \mathbb{E}_{\xi} [\|\mathbf{g}\|^2] \quad m_k = \frac{1}{\sqrt{d}} \mathbb{E}_{\xi} [\mathbf{g}^{\top} \mu_k]. \quad (46)$$

Observe that the equations above imply that $V_{\Delta} = v\Delta$ and $Q_{\Delta} = q\Delta$, where v and q are some constant that do not depend on Δ ¹. We can rewrite

$$v = \frac{\mathbb{E}_{\xi} [\mathbf{g}^{\top} \xi]}{d \sqrt{\hat{q}}} \quad (47a)$$

$$q = \frac{\mathbb{E}_{\xi} [\|\mathbf{g}\|^2]}{d} \quad (47b)$$

$$m_k = \frac{\mathbb{E}_{\xi} [\mathbf{g}^{\top} \mu_k]}{\sqrt{d}} \quad (47c)$$

and the remaining equations as

$$\hat{q} = \alpha \mathbb{E}_{k, \xi, \Delta} [\Delta f_k^2], \quad (48a)$$

$$\hat{v} = -\frac{\alpha}{\sqrt{\hat{q}}} \mathbb{E}_{k, \Delta, \xi} [\sqrt{\Delta} f_k \xi], \quad (48b)$$

$$\hat{m}_k = \alpha \rho_k \mathbb{E}_{\Delta, \xi} [f_k], \quad (48c)$$

$$b = \mathbb{E}_{k, \Delta, \xi} [h_k - m_k]. \quad (48d)$$

To obtain the replica symmetric free energy, therefore, the given set of equation has to be solved, and the result then plugged in Eq. (43).

A.2 Training and test errors

The order parameters introduced to solve the problem allow us to reach our ultimate goal of computing the average errors of the learning process. We will start with the estimation of the training loss. The complication in computing this quantity is that the order parameters found in the learning process are, of course, correlated with the dataset \mathcal{D} used for the learning itself. We need to compute the training loss

$$\epsilon_{\ell} \equiv \frac{1}{n} \sum_{\nu=1}^n \ell \left(y^{\nu}, \frac{\mathbf{w}^{\star} \mathbf{x}^{\nu}}{\sqrt{d}} + b^{\star} \right) \quad (49)$$

¹This was largely expected in our setting, but we preferred to keep a redundant derivation as this factorisation cannot be performed when the derivation is generalised to the case of non-diagonal random covariance matrices.

in the $n \rightarrow +\infty$ limit. The best way to proceed is to observe that

$$\mathbb{E}_{\mathcal{D}}[\mathcal{R}(\mathbf{w}^*, b^*)] = - \lim_{\beta \rightarrow +\infty} \mathbb{E}_{\mathcal{D}}[\partial_{\beta} \ln \mathcal{Z}_{\beta}] = \lambda \mathbb{E}_{\mathcal{D}}[r(\mathbf{w}^*)] + \epsilon_{\ell}$$

where

$$\epsilon_{\ell} = - \lim_{\beta \rightarrow +\infty} \partial_{\beta}(\beta \Psi_{\text{out}}) = \lim_{\beta \rightarrow +\infty} \mathbb{E}_{k, \Delta, \xi} \left[\int \frac{\ell_k(\eta) e^{-\frac{\beta(\eta - m_k^*)^2}{2\Delta v^*} - \beta \ell_k(\eta)}}{\sqrt{2\pi\beta^{-1}v^*\Delta} Z_k(\omega_k^*, \beta^{-1}v^*\Delta)} d\eta \right]. \quad (50)$$

In the $\beta \rightarrow +\infty$ limit, the integral concentrates on the minimizer of the exponent, that is, by definition, the proximal h_k . In conclusion, $\epsilon_{\ell} = \mathbb{E}_{k, \Delta, \xi}[\ell_k(h_k)]$. By means of the same concentration result, the training error is

$$\epsilon_t = \frac{1}{n} \sum_{\nu=1}^n \mathbb{I} \left(\varphi \left(\frac{\mathbf{w}^{*\top} \mathbf{x}^{\nu}}{\sqrt{d}} + b^* \right) \neq y^{\nu} \right) \xrightarrow{n \rightarrow +\infty} \mathbb{E}_{k, \Delta, \xi} [\mathbb{I}(\varphi(h_k) \neq y_k)]. \quad (51)$$

The expressions above hold in general, but, as anticipated, important simplifications can occur in the set of saddle-point equations (48) and (60) depending on the choice of the loss ℓ and of the regularization function r . The generalisation (or test) error can be written instead as

$$\epsilon_g = \mathbb{E}_{(y^{\text{new}}, \mathbf{x}^{\text{new}})} \left[\mathbb{I} \left(\varphi \left(\frac{\mathbf{w}^{*\top} \mathbf{x}^{\text{new}}}{\sqrt{d}} + b^* \right) \neq y^{\text{new}} \right) \right]. \quad (52)$$

This expression can be rewritten as

$$\begin{aligned} \epsilon_g &= \mathbb{E}_k \left[\int \mathbb{I}(\varphi(\eta) = y_k) \mathbb{E}_{\mathbf{x}^{\text{new}}} \left[\delta \left(\eta - \frac{\mathbf{w}^{*\top} \mathbf{x}^{\text{new}}}{\sqrt{d}} - b^* \right) \right] d\eta \right] \\ &= \mathbb{E}_{k, \Delta} \left[\int \mathbb{I}(\varphi(\eta) = y_k) \mathbb{E}_{\mathbf{x}^{\text{new}}|\Delta} \left[\delta \left(\eta - \frac{\mathbf{w}^{*\top} \mathbf{x}^{\text{new}}}{\sqrt{d}} - b^* \right) \right] d\eta \right] \\ &\xrightarrow{d \rightarrow +\infty} \mathbb{E}_{k, \Delta} \left[\int \mathbb{I}(\varphi(\eta) = y_k) \mathcal{N}(\eta | m_k^* + b^*, \Delta q^*) d\eta \right] \\ &= \mathbb{E}_{k, \Delta, \xi} \left[\mathbb{I} \left(\varphi \left(m_k^* + \sqrt{\Delta q^*} \xi + b^* \right) \neq y_k \right) \right]. \end{aligned} \quad (53)$$

This can be easily computed numerically once the order parameters (including their functional dependence on Δ) are given.

A.3 Ridge regularisation

Let us fix now $r(\mathbf{w}) = \frac{1}{2} \|\mathbf{w}\|^2$. In this case, the computation of $\Psi_{\mathbf{w}}$ can be performed explicitly via a Gaussian integration, and the saddle-point equations can take a more compact form that is particularly suitable for a numerical solution. In particular

$$\mathbf{g} = \frac{\sqrt{d} \sum_k \hat{m}_k \boldsymbol{\mu}_k + \sqrt{\hat{q}} \boldsymbol{\xi}}{\lambda + \hat{v}} \quad (54)$$

so that the prior saddle-point equations obtained from $\Psi_{\mathbf{w}}$ become

$$v = \frac{1}{\lambda + \hat{v}} \quad (55a)$$

$$q = \frac{\sum_{kk'} \hat{m}_k \hat{m}_{k'} \boldsymbol{\mu}_k^{\top} \boldsymbol{\mu}_{k'} + \hat{q}}{(\lambda + \hat{v})^2} \quad (55b)$$

$$m_k = \frac{\sum_{k'} \hat{m}_{k'} \boldsymbol{\mu}_{k'}^{\top} \boldsymbol{\mu}_k}{\lambda + \hat{v}}. \quad (55c)$$

Quadratic loss If we consider a quadratic loss $\ell(y, x) = \frac{1}{2} (y - x)^2$, then an explicit formula for the proximal can be found, namely

$$f_k = \frac{y_k - \omega_k}{1 + v\Delta} \quad (56)$$

so that the second set of saddle-point equations (48) can be written as

$$\hat{q} = \alpha \mathbb{E}_k [(y_k - m_k - b)^2] \mathbb{E}_\Delta \left[\frac{\Delta}{(1 + v\Delta)^2} \right] + \alpha q \mathbb{E}_\Delta \left[\frac{\Delta^2}{(1 + v\Delta)^2} \right], \quad (57a)$$

$$\hat{v} = \alpha \mathbb{E}_\Delta \left[\frac{\Delta}{1 + \Delta v} \right] = \frac{1 - v\lambda}{v}, \quad (57b)$$

$$\hat{m}_k = \alpha \rho_k (y_k - m_k - b) \mathbb{E}_\Delta \left[\frac{1}{1 + v\Delta} \right]. \quad (57c)$$

so that v satisfies the self-consistent equation

$$\frac{1 - v\lambda}{v\alpha} = \mathbb{E}_\Delta \left[\frac{\Delta}{1 + v\Delta} \right]. \quad (58)$$

Logistic loss We consider now the relevant case of the logistic loss $\ell(x) = \ln(1 + e^{-x})$. The proximal equation for this loss is the solution of the equations:

$$f_k \equiv \frac{h_k - \omega_k}{\Delta v}, \quad h_k = \arg \min_u \left[\frac{(u - \omega_k)^2}{2\Delta v} + \ln(1 + e^{-u}) \right]. \quad (59)$$

having only one solution for which, however, there is no closed-form expression; the equation can be solved numerically. To consider the $\lambda \rightarrow 0$ limit, it is convenient rescaling $\hat{v} \mapsto \lambda \hat{v}$, $v \mapsto \lambda^{-1}v$, $\hat{m} \mapsto \lambda^{-1}\hat{m}$, and $\hat{q} \mapsto \lambda^{-2}\hat{q}$. The prior equations become in this case

$$v = \frac{1}{1 + \hat{v}} \quad (60a)$$

$$q = \frac{\sum_{kk'} \hat{m}_k \hat{m}_{k'} \boldsymbol{\mu}_k^\top \boldsymbol{\mu}_{k'} + \hat{q}}{(1 + \hat{v})^2} \quad (60b)$$

$$m_k = \frac{\sum_{k'} \hat{m}_{k'} \boldsymbol{\mu}_{k'}^\top \boldsymbol{\mu}_k}{1 + \hat{v}}, \quad (60c)$$

so that they have no dependence on λ left. The channel part, instead, keeps the form in (48), but with proximal

$$f_k = \arg \min_u \left[\frac{\Delta v u^2}{2} + \lambda \ln \left(1 + e^{-\frac{\Delta v u + \omega_k}{\lambda}} \right) \right]. \quad (61)$$

Note that for $\lambda \rightarrow 0$, minimising the cross-entropy loss yields precisely the max-margin estimator [40].

B Note on the numerical results

Numerical experiments Numerical experiments regarding the quadratic loss with ridge regularisation were performed by computing the Moore-Penrose pseudoinverse solution. For the logistic loss, we used the `LogisticRegression` module from the `Scikit-learn` package [37].

State evolution equations Each average appearing in the update of the order parameters was performed using 10^5 instances of the variance. For the convergence criterion, we use a tolerance of 10^{-5} ; the algorithm stops and returns the parameters after at most 10^3 updates.

Note that, in the case of logistic regression, there are numerical instabilities when computing \hat{v} . To avoid them we first notice that $f_k + \partial_x \ell(\Delta v f_k + \omega_k) = 0$ holds, and we use this to compute $\partial_\omega f_k$ which we use in the application of Stein's lemma, rewriting the equation as

$$\hat{v} = -\frac{\alpha \mathbb{E}_{k,\Delta,\xi} \left[\sqrt{\Delta} f_k \xi \right]}{\sqrt{q}} = -\frac{\alpha \mathbb{E}_{k,\Delta,\xi} \left[\sqrt{\Delta} \partial_\xi f_k \right]}{\sqrt{q}} = \alpha \mathbb{E}_{k,\Delta,\xi} \left[\frac{\Delta \partial_x^2 \ell(\Delta v f_k + \omega_k)}{1 + \Delta v \partial_x^2 \ell(\Delta v f_k + \omega_k)} \right], \quad (62)$$

where $\partial_x^2 \ell(x) = [4(\cosh x/2)^2]^{-1}$ is the second derivative of the logistic loss. This equation is found to be much more stable.